Lab on a Chip

UniChip enables long-term recirculating unidirectional perfusion with gravity-driven flow for microphysiological systems

Journal:	*Lab on a Chip*
Manuscript ID	LC-ART-04-2018-000394.R1
Article Type:	Paper
Date Submitted by the Author:	21-Jun-2018
Complete List of Authors:	Wang, Ying; Cornell University, Meinig School of Biomedical Engineering Shuler, Michael; Cornell University, Meinig School of Biomedical Engineering

Title: UniChip enables long-term recirculating unidirectional perfusion with gravity-driven flow for microphysiological systems

Ying I. Wang[1] and Michael L. Shuler[1,2]

[1]Nancy E. and Peter C. Meinig School of Biomedical Engineering, Cornell University, Ithaca, NY, 14853, USA; [2]Robert Frederick Smith School of Chemical and Biomolecular Engineering, Cornell University, Ithaca, NY 14853, USA

Corresponding author: Michael L. Shuler

Address: 381 Kimball Hall

Ithaca, New York 14853-7202

Phone: 607 255-7577

Fax: 607 254-5375

E-mail: mls50@cornell.edu

Abstract

Microphysiological systems, also known as body-on-a-chips, are promising "human surrogates" that may be used to evaluate potential human response to drugs in preclinical drug development. Various microfluidics-based platforms have been proposed to interconnect different organ models and provide perfusion in mimicking the blood circulation. We have previously developed a pumpless platform that combines gravity-driven fluid flow and a rocking motion to create reciprocating flow between reservoirs for recirculation. Such platform allows design of self-contained and highly integrated systems that are relatively easy and cost-effective to construct and maintain. To integrate vasculature and other shear stress-sensitive tissues (e.g. lung and kidney) into pumpless body-on-a-chips, we propose "UniChip" fluid network design, which transforms reciprocating flow input into unidirectional perfusion in the channel(s) of interest by utilizing supporting channels and passive valves. The design enables unidirectional organ perfusion with recirculation on the pumpless platform and provides an effective backflow-proof mechanism. To demonstrate principles of UniChip design, we created a demonstration chip with a single straight channel as a simple example of the organ perfusion network. A BiChip providing bidirectional perfusion was used for comparison. Computational and experimental fluid dynamic characterization of the UniChip confirmed continuous unidirectional flow in the perfusion channel and the backflow-proof mechanism. Vascular endothelial cells cultured on UniChips for 5 d showed changes matching cell responses to unidirectional laminar flows. Those include cell elongation and alignment to the flow direction, continuous network of VE-cadherin at cell borders, realignment of F-actin and suppressed cell proliferation. Cells on BiChips manifested distinct responses that are close to responses to oscillatory flows, where cells remain a polygonal shape with intermittent VE-cadherin networks and few F-actin realignment. These

results demonstrate that microfluidic devices of UniChip design provide recirculating unidirectional perfusion suitable for long-term culture of shear stress-sensitive tissues. This is the first time a gravity-drive flow system has achieved continuous unidirectional perfusion with recirculation. The inherent backflow-proof mechanism allows hassle-free long-term operation of body-on-a-chips. Overall, our UniChip design provides a reliable and cost-effective solution for the integration of vasculature and other shear stress-sensitive tissues into pumpless recirculating body-on-a-chips, which can expedite the development and widespread application of moderately high-throughput, high-content microphysiological systems.

Keywords: pumpless; microphysiological systems; shear stress; unidirectional perfusion; gravity driven flow; endothelial cells; alignment;

Introduction

In vitro microscale biomimetics of the human body, namely, Body-on-a-Chip (BOC) microphysiological systems (MPS), are promising "human surrogates" to be used as in vitro models and tools for the next generation drug screening.[1] These systems integrate various tissue-engineered microscale organ models via microfluidic interconnections that mimic blood circulation.[1] Various microfluidic platforms have been proposed to enable organ perfusion and interconnection, providing continuous nutrient and oxygen supply, metabolic waste removal, and communication.[1] Sung et al., developed a pumpless platform that combines gravity-driven flow and a rocking motion to create fluid recirculation within a BOC model, allowing dynamic organ-organ interactions without the need for external pumps and tubing.[2] Such platform allows design of self-contained and highly integrated systems that are relatively easy and cost-effective to construct and maintain.[3] It has since been used for a variety of organ-on-a-chip models, including "skin", "liver", "gut" and "blood brain barrier", [4-7] as well as multiorgan microsystems of up to 13 organ models.[6, 8-12] Recently, the pumpless platform has also proved its great potential in supporting high content analysis in a relatively high throughput format.[6]

The pumpless platform of the original design achieves medium recirculation by creating reciprocating flow between a pair of reservoirs. Although such recirculation mode causes little deviation in the pharmacokinetic profiles of drugs compared to closed-loop unidirectional recirculation,[2] it induces oscillatory shear stress, which could potentially affect shear stress-sensitive tissues, such as the vasculature, kidney and lung. To better accommodate these tissues in a microfluidic MPS, several strategies have been proposed. In a microfluidic blood-brain barrier (BBB) model, Wang et al. utilized a "step chamber" that offset the culture plane of the barrier tissue from the channel plane by a distance to minimize the magnitude of bidirectional

shear stress on the cell surface.[7] This adaptation allowed brain microvascular endothelial cells (BMECs) to survive and maintain their unique BBB phenotype under reciprocating perfusion. In a pumpless gastrointestinal tract (GI)-liver MPS, Esch et al. designed a backflow channel and a set of passive valves to achieve semi-unidirectional perfusion.[8] Fluid circulating between a pair of reservoirs traveled alternately through the organ perfusion channel and the backflow channel. Such system provided unidirectional perfusion for a fraction of the period and halted flow for the rest of it. In contrast to bidirectional perfusion system, this GI-liver MPS was able to retain the barrier function of the GI tissue for at least 14 d.

To better incorporate the vasculature and other shear stress-sensitive tissues into BOC microsystems, we proposed a novel design of microfluidic network, the "UniChip" design, to achieve long-term reliable organ model perfusion with continuous unidirectional flow. The UniChip microfluidic network converts reciprocating flow input (e.g. gravity-driven flow on the pumpless platform) into continuous unidirectional perfusion in channel(s) of interest. By using a set of specially designed and routed supporting channels and valves, the UniChip design also provides an effective mechanism that prevents backflow in the perfusion channel(s). To show the principles of the UniChip design, we developed a demonstration device on the pumpless platform. Computational and experimental analysis of fluid dynamics of the demonstration UniChip confirmed continuous unidirectional flow and the backflow-proof mechanism in the perfusion channel. Vascular endothelial cells cultured on the UniChip device for 5 d underwent extensive cell remodeling, which matches cell responses to laminar flows, including cell elongation and alignment to the flow direction, continuous network formation of VE-cadherin, actin stress fiber formation and realignment, and suppressed cell proliferation. These are distinct from cell responses on a control device (BiChip) that provides bidirectional perfusion. We

further generalized the design principles of the UniChip to include multiple perfusion channels and allow more flexibility in channel design. We believe the UniChip design enables easy integration of shear stress-sensitive tissues onto the pumpless platform, allowing for hassle-free long-term operation of a BOC microphysiological system. The UniChip design can also be used for any application requiring unidirectional flow with recirculation.

Materials and Methods

1) System construction

The UniChip for demonstration has a microfluidic circuit (Figure 1A-B) comprising a pair of open-access reservoirs, a cell perfusion channel ("C_u"), and supporting channels ("a_1", "a_2", "b_1" and "b_2") with two integrated passive valves ("v_1" and "v_2").

Rapid prototype UniChips were fabricated mainly in poly(methyl methacrylate) (PMMA) using laser ablation and solvent assisted bonding techniques. The UniChip device consists of a top and a bottom piece with a cell insert and two side sealing sets sandwiched in between (Figure 1D). The top piece contains reservoirs and supporting channels and was made from five PMMA layers (Figure 1C): (i) reservoir walls; (ii) a reservoir base layer with openings connecting reservoirs to the supporting channels; (iii) b_1/b_2 channel layer (channel size: 1.4 mm × 1.5 mm × 26.3 mm, width × depth × length); (iv) a_1/a_2 channel layer (1.3 mm × 0.25 mm × 15.3 mm); and (v) a channel seal layer with openings connecting to the perfusion channel. All layers were cut and patterned from PMMA sheets (6mm, 3mm, or 1.5mm thickness, McMaster, Elmhurst, IL; 0.25mm thickness, Goodfellow, Coraopolis, PA) with a CO_2 laser (VersaLaser VLS3.50, the Universal Laser Systems, Scottsdale, AZ). Layer (ii)-(v) were permanently bonded

together via ethanol assisted thermal bonding [13]. Briefly, a thin layer of ethanol was applied to the bonding interface. PMMA layers were then aligned, placed into a preheated hot press (70°C), and held together with 1.2MPa pressure for 2 min. Reservoir walls were glued onto the reservoir base layer with a weld-on acrylic solvent cement (SCIGRIP, Durham, NC) to complete the top piece (Figure 1D). The bottom piece of the housing was also cut from PMMA sheets (6 mm) using laser ablation, and installed with screw-to-expand inserts for chip assembly.

The cell insert to accommodate endothelial cell cultures comprises a silicone perfusion channel layer with channel size of 0.76 mm × 0.25 mm × 6.25 mm (width × depth × length) and a cell culture coverslip (Figure 1D). The two sealing sets aside also comprise a silicone layer and a plastic coverslip. These silicone layers and the coverslips were patterned with the CO_2 laser from 0.25mm thick silicone sheets (Grace Bio-Labs, Bend, OR) and Thermanox plastic coverslips (Thermo Fisher, Waltham, MA), respectively. They were sterilized in 70% ethanol in DI water, aligned and assembled, and dried before used for experiment.

The BiChip providing bidirectional perfusion over cells contains three separate microfluidic circuits (Figure 1E). Each consists of a pair of reservoirs and a perfusion channel. The central segment of the BiChip channel (Figure 1E, C_b) is 0.76 mm × 0.25 mm × 6.25 mm (width × depth × length), and the side segments are 1.5 mm × 0.25 mm × 12.5 mm each. The housing and the cell insert were fabricated and prepared with the same materials and techniques used for the UniChips.

Static controls were assembled from a UniChip cell insert and a silicone ring, which were the reservoir walls of static chips and patterned with the CO_2 laser from a

2mm thick silicone sheet. All parts were sterilized in 70% ethanol in DI water, aligned and assembled, and dried before used for experiment.

2) Microfluidic channel design

The fluid flows on the UniChips and the BiChips are driven by gravity. The volumetric flow rate (Q) of a microfluidic channel follows Equation (1), where ΔP and R are the pressure drop and the hydrodynamic resistance, respectively.

$$Q = \frac{\Delta P}{R} \quad (1)$$

The dimensions of the UniChip microfluidic channels, including the perfusion and the supporting channels, were designed to achieve desired shear stress and flow rate in the UniChip perfusion channel (C_u). When the UniChip is placed on a tilted platform (e.g. +18°), valve v_1 is closed, and flow in channel b_1 is halted (Figure 1B). The flow rates in the other channels follow Equation set (2), where $\Delta P_{I_1 I_3}$ is the pressure drop between I/O ports, I_1 and I_3; and $\Delta P_{I_1 I_4}$ is that between I_1 and I_4 (Figure 1B). The pressure drops (ΔP) are determined by the height difference (Δh) between the top surface of fluid at the inlet and the outlet and can be calculated by Equation (3), where ρ and g are fluid density and the gravity constant. The hydrodynamic resistance for rectangular channels can be estimated by Equation (4), where μ is the dynamic fluid viscosity; l, w, and h ($h < w$) are the length, width and height of the channel, respectively. The resistance for the short tubular section at the entrance and exit connecting to the reservoirs can be estimated by Equation (5), where r and L are the radius and the length, respectively. Yet their resistance is usually negligible compared to the rest of the channel. For the desired Q and shear stress τ, channel dimensions were chosen to satisfy Equations (2) - (6).

$$\begin{cases} \Delta P_{I_1 I_3} = Q_{a_1} R_{a_1} + Q_{a_2} R_{a_2} \\ \Delta P_{I_1 I_4} = Q_{a_1} R_{a_1} + Q_{C_u}(R_{C_u} + R_{b_2}) \\ Q_{a_1} = Q_{a_2} + Q_{C_u} \end{cases} \quad (2)$$

$$\Delta P = \rho g \Delta h \quad (3)$$

$$R_{rectangular} = \frac{12\mu l}{wh^3}\left[1 - \frac{192h}{\pi^5 w} tanh\left(\frac{\pi w}{2h}\right)\right]^{-1} \quad (4)$$

$$R_{tubular} = \frac{8\mu L}{\pi r^4} \quad (5)$$

$$\tau = \frac{6\mu Q}{wh^2} \quad (6)$$

The BiChip was developed to provide bidirectional perfusion as a control flow condition. The aim for the BiChip microfluidic channel design was to create a bidirectional flow that runs at the same flow rate and exerts the same magnitude of shear stress on cells as the UniChip perfusion flow. To achieve that, we designed the central segments of the BiChip channels (Figure 1E, C_b) to share the same size (width × depth × length) as the UniChip perfusion channel (Figure 1B, C_u). We then designed the rest of the BiChip channels accordingly based on Equations (**1**), (**3**) and (**4**) so that the flow rate in the BiChip Channels is the same as that in C_u. According to Equation (**6**), with this design, the wall shear stress in C_b is also the same as that in C_u. Cells cultured in C_b and C_u are exposed to two flow conditions that share the same flow rate and wall shear stress, but differ in the flow direction.

3) Fluid dynamics simulation and characterization

The fluid dynamics in the demonstration UniChip devices and the BiChip controls were simulated in 3D using COMSOL Multiphysics to validate the microchannel design for the desired perfusion rate and wall shear stress. The Laminar Flow interface was used.

Gravity was applied as the only volume force. The steady state incompressible Navier-Stokes equations were used to model the fluid flow. The flow rate and the shear stress were derived from the velocity results. $\mu = 0.78\times10^{-3}$ Pa·s was used for culture medium at 37°C (Wang et al., 2013). The fluid dynamics were also characterized experimentally using colored food dyes for visualization. The maximum flow velocities in different channels were determined by timing the passage of dyes. Briefly, the device was placed on a 18° tilted platform. Phenol red free (colorless) medium was added to the upper position reservoir to flush though and fill all the channels. Medium was then removed from both reservoirs. Channels remained filled due to the capillary force. 90µl medium was added to the lower position reservoir, and 90µl medium mixed with a colored food dye was added to the upper reservoir. Fluid perfusion through channels was videotaped at 60 frames per second with a fix-positioned camera. Video frames were analyzed using ImageJ. A fixed threshold of color intensity was set to determine the moving dye front. Linear velocity was calculated by timing the moving dye front near the central streamline passing through a predetermined channel length (the entire C_u, the straight portion of a_1 or a_2, and a 5 mm straight channel marked on b_2). The experiments were conducted at room temperature (~20°C), thus the results were corrected for fluid viscosity at room temperature ($\mu = 1.00\times10^{-3}$ Pa·s) before compared to the designed or simulation values.

4) Cell culture

Cryopreserved human umbilical vein endothelial cells (HUVECs) from Lonza (Walkersville, MD) were recovered and expanded in Endothelial Cell Growth Medium-2 (EGM-2, Lonza) and maintained at 37°C with 5% CO_2 in a humidified cell culture incubator. Cells were passaged at 80% confluence with TrypLE Express (Thermo Fisher) and used for experiments at

passage 6. 1× Penicillin–Streptomycin (Thermo Fisher) was supplemented to culture medium for experiments.

5) Device assembly and operation

HUVEC cultures on cell inserts were first prepared in culture dishes (Figure 1F). Cell culture area was coated with a mixture of collagen IV (50 μg/mL, Sigma-Aldrich, St. Louis, MO) and fibronectin (12.5 μg/ mL, Sigma-Aldrich) in DPBS (Thermo Fisher), and incubated at 37 °C for 1 hour. The coating solution was then removed and the coated area was rinsed with DPBS. HUVECs were seeded onto cell inserts at density of 100K/cm^2, and maintained in static culture dishes for 24 h to allow for cell settlement and attachment prior to transferring to the onchip systems. UniChips and BiChips were assembled by sandwiching a cell-loaded insert between a top and a bottom piece of the housing and securing with screws. Each reservoir was filled with 90 μl culture medium (180 μl per pair of reservoirs), and capped with lid made from breathable polyurethane membranes (Sigma-Aldrich) to minimize evaporation. The assembled Unichips and BiChip were placed on a rocking platform (Next Advance, Averill Park, NY) that was custom programmed to tilt at +18° or -18° during a 15-s interval and flipped quickly to the opposite tilt direction at the end of each interval. The whole system was placed inside a 5% CO_2 cell culture incubator. The static controls remained in static culture dishes with each reservoir filled with 180 μl culture medium. For all chips, medium was replenished daily.

6) Immunofluorescence microscopy

Phase contrast micrographs of live cell morphology were acquired with an inverted microscope (Olympus) right before device assembly and daily after assembly for 5 days. Cells were then analyzed by immunofluorescence staining for VE-cadherin and actin filaments (F-actin). Staining was carried out at room temperature. Cells were fixed with Image-iT™ Fixative

Solution (4% paraformaldehyde, Thermo Fisher) for 10 min, washed with DPBS (Thermo Fisher), permeabilized with 0.1% Triton X-100 (Sigma-Aldrich) in DPBS for 10 min, blocked with 5% bovine serum albumin (BSA) blocking buffer (Alfa Aesar, Haverhill, MA) for 1 hour, and then incubated with Alexa Fluor 488 conjugated VE-cadherin monoclonal antibody (4 µg/mL, Santa Cruz Biotechnology, Dallas, TX) and Cruzfluor 555 conjugated phalloidin (1 µg/mL, Santa Cruz Biotechnology) in 1% BSA for 2 hours. Samples were then washed 3 times in DPBS and mounted on slides with Fluoroshield™ with DAPI (Sigma-Aldrich) for nuclear counterstain. Images were captured with a Zeiss LSM 710 confocal microscope and analyzed in ImageJ. Visual orientation analysis on cell actin filaments was performed using an ImageJ directional analysis plugin – OrientationJ[14]. Cells were counted based on nuclear staining.

7) Statistical analysis

Data are presented as mean ± SD. Multiple groups were analyzed by one-way ANOVA with Tukey's multiple comparisons test (GraphPad Prism). $p < 0.05$ was considered significant.

Results and discussion

1. Design and operation of a demonstration UniChip device on the pumpless platform

We propose a novel design of microfluidic networks, so called UniChip, to adapt the pumpless MPS platform for shear stress-sensitive cells and organ models. By utilizing a set of specially designed and routed supporting channels and valves, UniChip microfluidic networks convert reciprocating gravity-driven flows on the pumpless platform into continuous unidirectional perfusion through organ models. More importantly, the design is integrated with a backflow-proof mechanism that ensures the unidirectionality of flows in the organ perfusion channel(s).

We have developed a simple UniChip device for demonstration, as illustrated in Figure 1A-D. The device was designed to provide unidirectional perfusion from "A" to "B" in channel C_u (Figure 1A), which is a straight rectangular microfluidic channel used for organ perfusion (Figure 1B). Channels a_1, a_2, b_1, and b_2 are supporting channels that connect C_u to reservoirs. A pair of reservoirs on a tilted rocking platform were used to provide reciprocating flow input. Valves v_1 and v_2 are two 0.4 mm diameter tubular channels connecting reservoirs to channel b_1 or b_2 (Figure 2) and operate passively by capillary forces. Briefly, when the pumpless platform is tilted clockwise by 18° (Figure 2A), a liquid-air interface forms in v_1. The capillary force retains fluid in v_1 if the elevation difference between two reservoirs does not exceed the capillary rise (h) it can support. Capillary rise h can be calculated from Equation (**7**). Flow in channel b_1 is thus halted. Gravity drives flow from Reservoir I to Reservoir II through channels a_1, C_u, b_2, and a_2. Similarly, when the platform flips counterclockwise (Figure 2B), a liquid-air interface forms in v_2 and prevents backflow in channel b_2. Fluid returns to Reservoir I though a_2, C_u, b_1, and a_1. In both cases, the flow direction in channel C_u remains the same (green arrows).

$$h = 2\,\gamma\,cos\theta\,/\,\rho g r \tag{7}$$

r is the radius of a cylindrical channel, θ is the contact angle, and γ is the liquid-air surface tension.

The design of the UniChip device prevents backflow in the perfusion channel in cases where excessive fluid in the reservoirs covers the valves (Figure 3, Reservoir I), and delays liquid-air interface formation when the platform flips. In such scenarios, the fluidic network structure is altered, and the flow rates in different channels are governed by a new set of Equations (8). A positive flow rate value means that the flow direction is the same as shown in Figure 3. The pressure drops (ΔP) can be calculated by Equations (9), where Δh_1 and Δh_2 are

the height differences between the top surface of fluid at the inlets and the outlets (Figure 3). We then derive Q_{C_u} as shown by Equation (10). As $\Delta h_2 \geq \Delta h_1$ (equal when both valves are covered in medium), we can find a lower limit for Q_{C_u} as stated in Inequality (11). The dimensions of channels a_1 and b_1 are identical to those of a_2 and b_2, respectively, so are their hydraulic resistance, that is, $R_{a_1} = R_{a_2}$ and $R_{b_1} = R_{b_2}$. Therefore, the lower limit for Q_{C_u} is 0, meaning no backflow occurs in C_u. This remains true for an oppositely tilted situation. In fact, as long as $\frac{R_{a_2}}{R_{b_2}} = \frac{R_{a_1}}{R_{b_1}}$ is satisfied, backflow in C_u is prevented. An even more generalized form of the UniChip design will be described and discussed in detail in section 4.

$$\begin{cases} \Delta P_{I_1 I_3} = Q_{a_1} R_{a_1} + Q_{a_2} R_{a_2} \\ \Delta P_{I_2 I_4} = Q_{b_1} R_{b_1} + Q_{b_2} R_{b_2} \\ \Delta P_{I_1 I_4} = Q_{a_1} R_{a_1} + Q_{C_u} R_{C_u} + Q_{b_2} R_{b_2} \\ Q_{a_1} = Q_{a_2} + Q_{C_u} \\ Q_{b_2} = Q_{b_1} + Q_{C_u} \end{cases} \tag{8}$$

$$\begin{cases} \Delta P_{I_1 I_3} = \rho g \Delta h_1 \\ \Delta P_{I_2 I_4} = \rho g \Delta h_2 \\ \Delta P_{I_1 I_4} = \rho g \Delta h_2 \end{cases} \tag{9}$$

$$Q_{C_u} = \frac{\rho g}{\frac{R_{a_1} R_{a_2}}{R_{a_1} + R_{a_2}} + R_{C_u} + \frac{R_{b_1} R_{b_2}}{R_{b_1} + R_{b_2}}} \left(\frac{R_{b_1}}{R_{b_1} + R_{b_2}} \Delta h_2 - \frac{R_{a_1}}{R_{a_1} + R_{a_2}} \Delta h_1 \right) \tag{10}$$

$$Q_{C_u} \geq \frac{\rho g \Delta h_1}{\frac{R_{a_1} R_{a_2}}{R_{a_1} + R_{a_2}} + R_{C_u} + \frac{R_{b_1} R_{b_2}}{R_{b_1} + R_{b_2}}} \cdot \frac{R_{b_1} R_{b_2}}{(R_{b_1} + R_{b_2})(R_{a_1} + R_{a_2})} \left(\frac{R_{a_2}}{R_{b_2}} - \frac{R_{a_1}}{R_{b_1}} \right) \tag{11}$$

2. Computational and experimental analysis of fluid dynamics confirms unidirectional perfusion

The flow rate and shear stress are dynamic in an operating device, varying with the tilt angle and the fluid level difference between the two reservoirs. We have designed a rocking motion with rapid flipping of tilt direction between intervals to maximally maintain the device at a constant tilt angle. Such rocking motion, compared to those with continuously changing tilt angle in our previous systems,[5] can largely reduce flow rate fluctuation. In addition, we have designed the reservoirs to have a relatively large bottom area to minimize variation of inter-reservoir fluid level difference due to fluid transport between reservoirs, and thus the pulsatility of flow rates. Microfluidic channel dimensions were chosen to achieve desired flow rate and shear stress. To verify the channel design, we performed computational and experimental analysis of an average steady-state flow condition, where the device is tiled at 18° and each reservoir holds equivalent amount of medium. We simulated the fluid dynamics of the demonstration UniChip through finite element analysis of the fluid velocity (Figure 4A i). The flow rates and shear stress derived from the simulated velocity field closely match the design values (Figure 4A ii-iii). The maximum flow velocity at the center streamline for each channel in an operating device was experimentally determined by measuring the linear velocity of a moving dye front. After corrected for fluid viscosity difference (1.00×10^{-3} Pa·s for flow experiments at 20°C vs. 0.78×10^{-3} Pa·s for culture at 37°C), the velocity results of all channels were within ±1~4% of the simulated values (Figure 4A iv). We acknowledge that the accuracy of dye based velocity measurement can be affected by the diffusion of dyes used for visualization. However, we consider such effect almost negligible in the current experiment, due to the short period needed for flow to pass through each timed distance (0.15 ~ 1.2s). The diffusion coefficient of a typical food coloring dye is around 200 $\mu m^2/s$.[15] The diffusion distance over 1s is around 0.02 mm. Compared to the measured velocities ranging from 4 to 42 mm/s (at room temperature), the

effect of dye diffusion is negligible. Our results validate the design of UniChip channel dimensions and suggest that the desired fluid dynamics were recreated in the fabricated device.

We next tested the unidirectionality of perfusion of the demonstration UniChip. Red dye placed in one reservoir flowed to the other reservoir through the top (a_1, a_2), center (C_u) and bottom (b_1) channels (Figure 4B). Once the device was flipped (Figure 4C), blue dye replacing red dye in the other reservoir flowed back to the initial reservoir through the top (a_1, a_2), center (C_u) and bottom (b_2) channels. Unidirectional flow was thus achieved within the center channel as shown by the black arrows. To test the backflow proof mechanism of the UniChip design in cases where valves fail or delay to close, we placed excessive fluid (purple dye) in the top reservoir that completely covered the passive valve and delayed the liquid-air interface formation (Figure 4D). Purple dye flows to the other reservoir through the top (a_1, a_2) and the bottom channels (b_1, b_2). It only started to flow through the center channel in the designed perfusion direction (ii. black arrow) when the interface began to form. During the whole time, no backwards flow was observed. Together these results suggest that the demonstration UniChip can provide unidirectional perfusion at desired flow rate and shear stress with an integrated mechanism preventing backwards perfusion.

3. HUVEC responses on UniChip differ from those on BiChips, matching cell responses under unidirectional laminar perfusion

We next evaluated the application of UniChip devices for long-term dynamic culture of shear stress-sensitive tissues. We used endothelial cells (ECs) for testing purpose. ECs lining the inner layers of the vasculature are directly exposed to hydrodynamic forces (e.g. shear stress induced by blood flow) that have been shown to modulate endothelial proliferation, function and

inflammatory phenotype.[16] Disturbed flow profiles often correlate with the localization of elevated inflammation and atherosclerotic lesions.[16]

We seeded HUVECs on the cell inserts of Unichip and BiChip devices at a same density and assembled all devices 24 hr later (day 0, Figure 5a-b). To assess the impact of a longer duration of shear stress exposure rather than the transient response to the onset of flow, we maintained the cultures onchip for 5 days. The magnitude of shear stress acting on the ECs was estimated to be 5.3 dyne/cm^2 (Figure 4A iii). Visible remodelling of endothelial monolayers on the UniChip devices was observed by phase contrast microscopy by day 3. That became clearly significant by day 5 (Figure 5c). Endothelial cells were elongated and aligned in the direction of flow, matching EC morphology under laminar flow[17]. In contrast, endothelial cells exposed to bidirectional perfusion on the BiChips remained a polygonal shape as seen in static culture, and showed no evident preference for orientation (Figure 5d).

We next investigated the expression and distribution of VE-cadherin, an endothelial specific adhesion molecule at the cell-cell junctions that modulates endothelial permeability. It is a major player in the mechanosensory complex and is considered responsible for cellular response to shear stress.[18] Immunofluorescence staining revealed strong expression of VE-cadherin (green) at cell-cell junctions in both the UniChip and the BiChip cultured HUVECs (Figure 5e-f). The distribution or network organization of VE-cadherin in the two EC cultures, however, was different, as shown in the zoomed-in insets. These results reflect cell junction remodeling and differential redistribution of VE-cadherin in response to different flow patterns. They are consistent with in vivo observations of stronger pericellular staining of VE-cadherin at locations associated with pulsatile flow with net forward component than at places with complex

and reciprocating flow.[19] They are also in line with in vitro studies that showed continuous versus intermittent staining of VE-cadherin under laminar versus reciprocating flows.[16, 19]

Endothelial remodeling also involves reorganization of actin filaments (F-actin). We visualized F-actin organization using confocal microscopy with fluorophore conjugated phalloidin. Long and thick stress fibers were observed in the central areas of ECs cultured on UniChips and were oriented parallel to the flow direction (Figure 5g, i), while short and thin filaments randomly orientated and presented mostly at cell periphery in cells cultured on BiChips (Figure 5h, j). For further visual and quantitative analysis of F-actin alignment, we used an ImageJ directional analysis plugin – OrientationJ[14]. The HSB (Hue: local orientation; Saturation: coherency; Brightness: from the original image) color coded maps of representative F-actin staining images confirmed F-actin alignment to the flow direction (0°, Figure 6a) in UniChip perfused ECs, and more random orientation in BiChip cultured ECs (Figure 6b). The dominant orientation of actin filaments in each cell was also analyzed with OrientationJ. The results for 2000 cells of each group were summarized in Figure 6c-d. The distribution of endothelial F-actin orientation for the UniChip group fits a Gaussian curve with a mean around 0° and a standard deviation of 15.6°. A quarter of the EC population were oriented within ±5° of the flow direction, 63% within ±15°, and 82% within ±25°. For the BiChip group, although the F-actin orientation looked random by eyes, the quantitative analysis shows that it also follows a Gaussian distribution with a mean around 0, but the distribution is much broader with a larger standard deviation of 44.9°. Only 10% of ECs were oriented within ±5° of the flow direction, 28% within ±15°, and 43% within ±25°. UniChip perfusion for 5 days led to a majority of HUVEC F-actin aligning to the flow direction, while such realignment was much subtler in the population under oscillatory perfusion on BiChips. Our observations of actin remodeling for cell

alignment under UniChip or BiChip perfusion match those under laminar or oscillating disturbed flow.

In addition, although EC monolayers in all groups were confluent on day 5, the cell density differed among UniChip, BiChip or static dish cultured EC populations. There was no significant difference in the averaged cell densities from 10 representative views (567μm × 567μm each) for the BiChip group (Figure 7, 70004 ± 1073 cells/cm^2) and the static control (74591± 2368 cells/cm^2). However, the number for the UniChip group was about 40% lower (44728 ± 1073/cm^2) compared to the other two groups. These results are not unexpected as laminar flow has been shown to restrict EC proliferation by suppressing cell transition from the G(1) to S phase of the cell cycle,[20, 21] while disturbed flow with reciprocating shear stress enhances EC proliferation and migration that often increase endothelial permeability.[16]

In summary, the recirculating perfusion provided by UniChips elicited similar endothelial cell response as to unidirectional laminar flows. We observed cell elongation and alignment to the direction of flow, continuous VE-cadherin network formation at the cell borders, actin stress fiber formation and realignment to flow, and lower cell density in UniChip cultured ECs. These observations are in line with previously reported EC responses to laminar shear stress achieved with pumps[17] or cone-and-plate devices[22], yet are distinct from our observations for BiChip cultured ECs or previously reported cell responses to oscillating disturbed flows[16].

4. General form of the UniChip design

We have demonstrated a simple UniChip device with a single perfusion channel. In fact, the UniChip design that transforms reciprocating flow input into unidirectional perfusion can be extended in general terms to include multiple perfusion channels and allow more flexibility in channel design.

A general form of UniChip microfluidic network comprises a pair of inlet/outlet (Figure 8, "O_1" and "O_2") that receives reciprocating flow input, one or more unidirectional channel networks (UCNs) for organ perfusion, and a supporting fluid channel network (SCN). The design is detailed below.

i. Each UCN comprises at least one fluid channel. The i^{th} UCN is denoted by "U_i". Its inlet and outlet are denoted by "A_i" and "B_i", respectively.

ii. The SCN comprises fluid channel networks connecting the inlets or outlets of neighboring UCNs and the UniChip inlet/outlet ("O_1" or "O_2").

- The connecting fluid channel networks between the inlets of UCNs and the UniChip inlet/outlet (O_1 or O_2) are denoted by "a_1", "a_2", …, and "a_{n+1}" ($n \geq 0$, integer); the corresponding hydraulic resistance of a_j ($j = 1, 2, \ldots, n+1$) is R_{a_j};
- The connecting fluid channel networks between the outlets of UCNs and the UniChip inlet/outlet (O_1 and O_2) are denoted by "b_1", "b_2", …, and "b_{n+1}"; the corresponding hydraulic resistance of b_j ($j = 1, 2, \ldots, n+1$) is R_{b_j};
- Each connecting fluid channel network (a_j or b_j) comprises at least one fluid channel.
- b_1 and b_{n+1} each contain at least one valving device. The valving device(s) can be any device that has different statuses (open, close or changed hydraulic resistance of specific channels) for different flow direction (towards or away from the nearby UniChip inlet/outlet (O_1 or O_2)), such as check valves and multi-way valves. $R_{b_i}^{+}$ is the overall hydraulic resistance

of b_i (i = 1, n+1) when fluid flows towards the neighboring inlet/outlet (O_1 or O_2), and $R_{b_i}^-$ is that when fluid flows away from the neighboring inlet/outlet (O_1 or O_2); $R_{b_i}^+ < R_{b_i}^-$;

UCNs can maintain continuous unidirectional flow ($A_i \rightarrow B_i$ with no backflow) even when inlet and outlet (O_1 and O_2) swaps if Equation (7) is satisfied. All fluid channels can otherwise be of any length and shape (such as rectangular, trapezoidal, circular, or irregular shapes). Under such design constraints, flows in UCNs remain unidirectional even when the valving device in b_i (i = 1, n+1) fails to limit backwards flow (i.e., decreased $R_{b_i}^-$). In extreme scenarios where the valving device completely fails ($R_{b_i}^-$ decreases to as low as $R_{b_i}^+$), there would be no pressure drop between A_j and B_j in a steady state, thus no flow in the UCNs. If during transition period $R_{b_i}^-$ drops close to $R_{b_i}^+$, the flow in UCNs will just be approaching 0, but do not flow backwards.

$$\frac{R_{a_1}}{R_{b_1}^+} = \frac{R_{a_j}}{R_{b_j}} = \cdots = \frac{R_{a_{n+1}}}{R_{b_{n+1}}^+}, j = 1, 2, \ldots, n+1; \quad (12)$$

An example multi-channel, multi-unit UniChip is illustrated in Supplement Figure 1. The fluid network includes two UCNs, U_1 with 3 branching channels and U_2 with 4. $\boldsymbol{\frac{R_{a_1}}{R_{b_1}} = \frac{R_{a_2}}{R_{b_2}} = \frac{R_{a_3}}{R_{b_3}}}$ is achieved by designing channels a_i and b_i to have same length and width but different depth (i=1, 2, or 3). v_1 and v_2 are one-way valves, which only allow flow in b_1 from B_1 to O_1 or flow in b_3 from B_2 to O_2. Computational simulation of the velocity field confirmed the unidirectionality of flows in U_1 and U_2 with reciprocating flow input between O_1 and O_2 (Supplement Figure 2). In cases where one-way valves completely fail to limit backwards flow (e.g. v_1 fails to limit flow

in b_1 from O_1 to B_1), the flow rates in U_1 and U_2 decrease to approaching 0 but do not flow backwards (Supplement Figure 3).

Concluding remarks

We proposed UniChip, a novel design of fluidic networks, to achieve continuous unidirectional perfusion with recirculation in pumpless microphysiological systems. A simple UniChip device with one single perfusion channel was developed for demonstration, and generalized design principles of the UniChip were described in detail. Computational and experimental analysis of the fluid dynamics of the UniChip device confirmed the unidirectionality of the flow and the backflow-proof mechanism in the perfusion channel. To our knowledge, this is the first time that continuous unidirectional perfusion with recirculation is achieved in a gravity-driven flow system.

We demonstrated that UniChip devices are suitable for long-term culture of shear stress-sensitive tissues. Endothelial cells cultured on UniChips for 5 days exhibited similar cell remodeling as seen in response to laminar flows driven by pumps. The 5-day period of dynamic culture was chosen to study long-term effects of shear stress exposure rather than flow onset, but the UniChip system itself can easily operate for much longer period. Fault-tolerance is particularly sought after in the design of pumpless UniChip devices for long-term tissue culture. The backflow-proof mechanism embedded in the supporting channel design ensures reliable unidirectional perfusion even when passive valves fail (e.g. delayed shut-off due to excessive fluid in the reservoirs). The tubular channels (passive valves and the inlet/outlet) connecting to the reservoirs not only contribute to creating the unidirectional perfusion, but also prevent fluid depletion in the perfusion channel(s) in cases where reservoirs are depleted (e.g. excessive

evaporation or prolonged holding time at one tilting direction). All these enable a hassle-free operation for long-term perfusion of organ models, especially shear stress-sensitive tissues.

We believe the UniChip design provides a reliable and cost-effective solution for the integration of vasculature and other shear stress-sensitive tissues (e.g. lung and kidney) into pumpless recirculating body-on-a-chip systems. The single perfusion channel in the demonstration UniChip can be replaced with more complicated microfluidic networks that have branches for multiple organ perfusion. We have currently developed prototypes of multi-channel, multi-organ UniChip systems. The symmetric microfluidic network structure can also be replaced with asymmetric design to achieve pulsatile perfusion if desired. The open reservoirs provide easy access for medium sampling and exchange in a recirculating fluid system, as compared to closes-loop fluid systems driven by pneumatic or peristatic pumps. We believe incorporation of UniChip design into the pumpless platform can expedite the development and widespread application of moderately high-throughput, high-content microphysiological systems.

Of note, although UniChip design was initially proposed on a pumpless platform, itself is not limited to gravity-driven fluid systems. It can be used to derive continuous unidirectional flow from any reciprocating flow input. In addition, although the UniChip was inspired to solve challenges in microfluidic tissue culture, its application is not limited to microphysiological systems. It can be used for any application requiring unidirectional flow with recirculation. Examples include sequential localized heating with multiple cycles, or onchip cell metabolite sensing with sequential enzymatic reactions and subsequent detection, or even nonbiological applications.

Acknowledgments

This work was performed in part at the Cornell NanoScale Science and Technology Facility, a member of the National Nanotechnology Coordinated Infrastructure (NNCI) network, which is supported by the National Science Foundation (grant ECCS-1542081). This work was also supported in part by NIH grants 1U01CA214300-01A1 and 5R44 TR001326-02.

References

1. Y. I. Wang, C. Carmona, J. J. Hickman and M. L. Shuler, *Adv Healthc Mater*, 2018, 7.
2. J. H. Sung, C. Kam and M. L. Shuler, *Lab Chip*, 2010, 10, 446-455.
3. Y. I. Wang, C. Oleaga, C. J. Long, M. B. Esch, C. W. McAleer, P. G. Miller, J. J. Hickman and M. L. Shuler, *Exp Biol Med (Maywood)*, 2017, 242, 1701-1713.
4. H. E. Abaci, K. Gledhill, Z. Guo, A. M. Christiano and M. L. Shuler, *Lab Chip*, 2015, 15, 882-888.
5. M. B. Esch, J. M. Prot, Y. I. Wang, P. Miller, J. R. Llamas-Vidales, B. A. Naughton, D. R. Applegate and M. L. Shuler, *Lab Chip*, 2015, 15, 2269-2277.
6. S. J. Trietsch, E. Naumovska, D. Kurek, M. C. Setyawati, M. K. Vormann, K. J. Wilschut, H. L. Lanz, A. Nicolas, C. P. Ng, J. Joore, S. Kustermann, A. Roth, T. Hankemeier, A. Moisan and P. Vulto, *Nat Commun*, 2017, 8, 262.
7. Y. I. Wang, H. E. Abaci and M. L. Shuler, *Biotechnol Bioeng*, 2017, 114, 184-194.
8. M. B. Esch, H. Ueno, D. R. Applegate and M. L. Shuler, *Lab Chip*, 2016, 16, 2719-2729.
9. P. G. Miller and M. L. Shuler, *Biotechnol Bioeng*, 2016, 113, 2213-2227.
10. C. Oleaga, C. Bernabini, A. S. Smith, B. Srinivasan, M. Jackson, W. McLamb, V. Platt, R. Bridges, Y. Cai, N. Santhanam, B. Berry, S. Najjar, N. Akanda, X. Guo, C. Martin, G. Ekman, M. B. Esch, J. Langer, G. Ouedraogo, J. Cotovio, L. Breton, M. L. Shuler and J. J. Hickman, *Sci Rep*, 2016, 6, 20030.
11. A. Choe, S. K. Ha, I. Choi, N. Choi and J. H. Sung, *Biomed Microdevices*, 2017, 19, 4.
12. H. Lee, D. S. Kim, S. K. Ha, I. Choi, J. M. Lee and J. H. Sung, *Biotechnol Bioeng*, 2017, 114, 432-443.
13. A. M. Wan, T. A. Moore and E. W. Young, *J Vis Exp*, 2017, DOI: 10.3791/55175.
14. E. Fonck, G. G. Feigl, J. Fasel, D. Sage, M. Unser, D. A. Rufenacht and N. Stergiopulos, *Stroke*, 2009, 40, 2552-2556.
15. B. Giri, *Laboratory methods in microfluidics*, Elsevier, Waltham, MA, 1st edition. edn., 2017.
16. J. J. Chiu and S. Chien, *Physiol Rev*, 2011, 91, 327-387.
17. M. J. Levesque and R. M. Nerem, *J Biomech Eng*, 1985, 107, 341-347.
18. B. G. Coon, N. Baeyens, J. Han, M. Budatha, T. D. Ross, J. S. Fang, S. Yun, J. L. Thomas and M. A. Schwartz, *J Cell Biol*, 2015, 208, 975-986.
19. H. Miao, Y. L. Hu, Y. T. Shiu, S. Yuan, Y. Zhao, R. Kaunas, Y. Wang, G. Jin, S. Usami and S. Chien, *J Vasc Res*, 2005, 42, 77-89.
20. S. Akimoto, M. Mitsumata, T. Sasaguri and Y. Yoshida, *Circ Res*, 2000, 86, 185-190.
21. M. J. Levesque, R. M. Nerem and E. A. Sprague, *Biomaterials*, 1990, 11, 702-707.
22. M. Franzoni, I. Cattaneo, B. Ene-Iordache, A. Oldani, P. Righettini and A. Remuzzi, *Cytotechnology*, 2016, 68, 1885-1896.

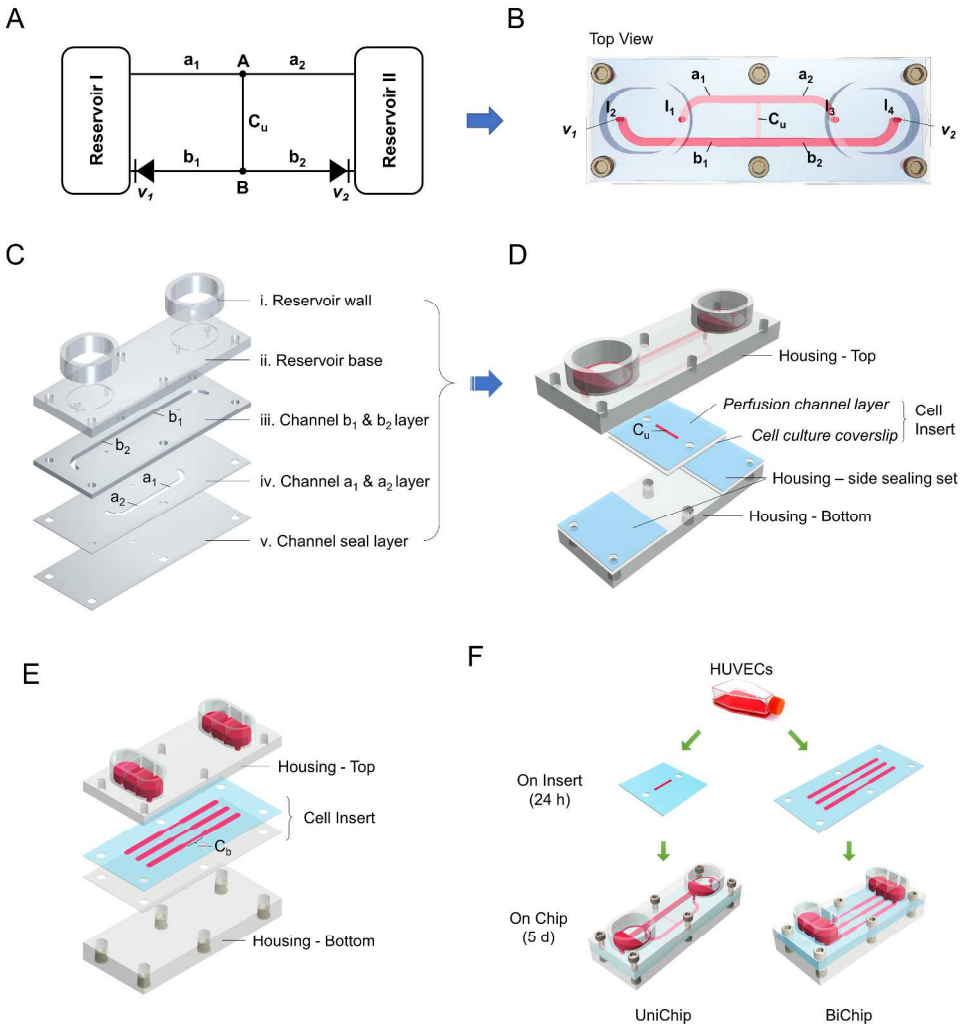

Figure 1 System construction and assembly. Microfluidic circuit diagram of the demonstration UniChip (A), and the top view of the device (B). C_u, perfusion channel; a_1, a_2, b_1, and b_2, supporting channels; v_1, v_2, passive valves. The top piece of the housing containing reservoirs and supporting channels were constructed from patterned PMMA layers (C). A cell insert composed of a silicon perfusion channel layer and a cell culture coverslip was sandwiched between the top and bottom pieces of the housing for assembly (D). (E) Schematic exploded view of the BiChip, which contains 3 sets of microfluid circuits, each with a pair of reservoirs and a perfusion channel. (F) HUVECs were seeded onto inserts and cultured for 24 h before assembling the cell inserts onto chips (UniChips or BiChips). They were all maintained onchip for 5 days.

401x421mm (300 x 300 DPI)

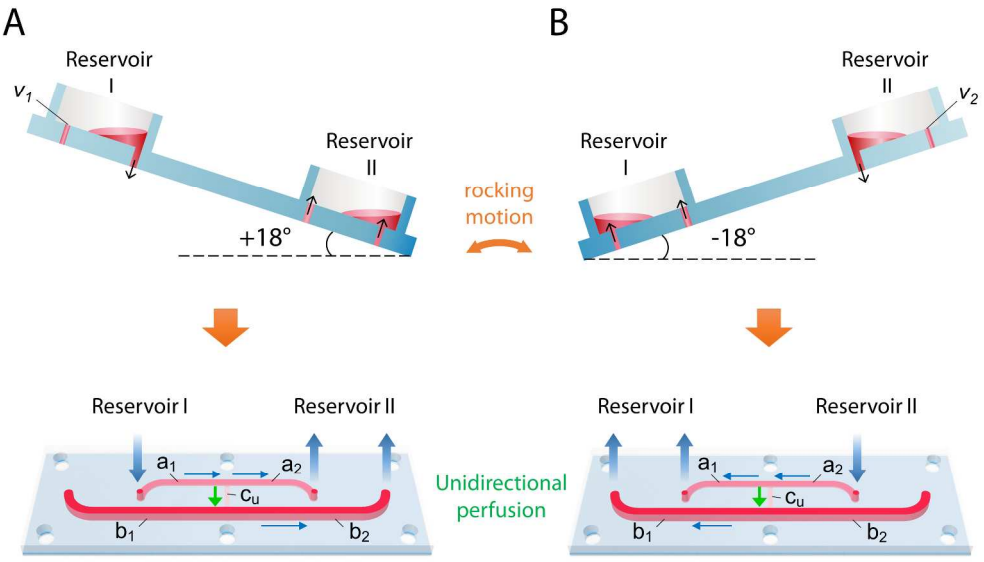

Figure 2 Schematic of UniChip operation. A demonstration UniChip is placed on a rocker platform that flips tilting between +18° (A) and -18° (B) periodically. When tilted at +18° (A), flow in b_1 is halted by the capillary force at the air-liquid interface in the passive valve v_1. Flow is directed from Reservoir I through a_1, a_2, C_u and b_2 into Reservoir II. When tilted at -18° (B), flow in b_2 is halted by valve v_2, and flow is directed from Reservoir II through a_2, a_1, C_u and b_1 into Reservoir II. Under either condition, the flow direction in the cell perfusion channel, C_u, is kept the same, shown by the green arrows.

254x144mm (300 x 300 DPI)

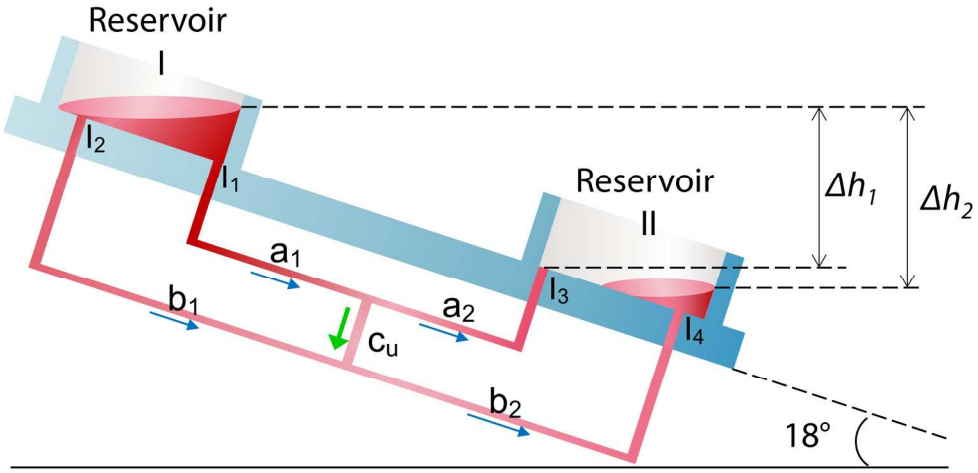

Figure 3. Schematic illustration of the fluid channel network in the demonstration UniChip device. The diagram is to show the network structure including connections among different channels not the actual channel dimensions. The pressure drop between different I/O ports is determined by the fluid level difference. Δh_1 between I_1 and I_3; Δh_2 between I_2 and I_4, and between I_1 and I_4.

177x88mm (300 x 300 DPI)

A

i

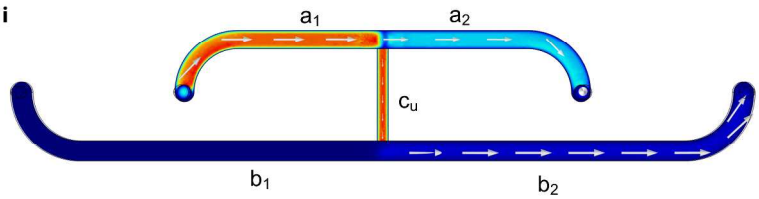

ii

	Flow rate (µl/min)	
	Design	*Simulation*
a_1	568.7	562.0
C_u	320.9	319.6

iii

	Shear stress (dyne/cm²)	
	Design	*Simulation*
C_u	5.3	5.3

iv

	Velocity (mm/s)	
	Simulation	*Measurement*
a_1	50.24	52.2
a_2	22.11	22.4
C_u	52.40	52.9
b_2	5.35	5.5

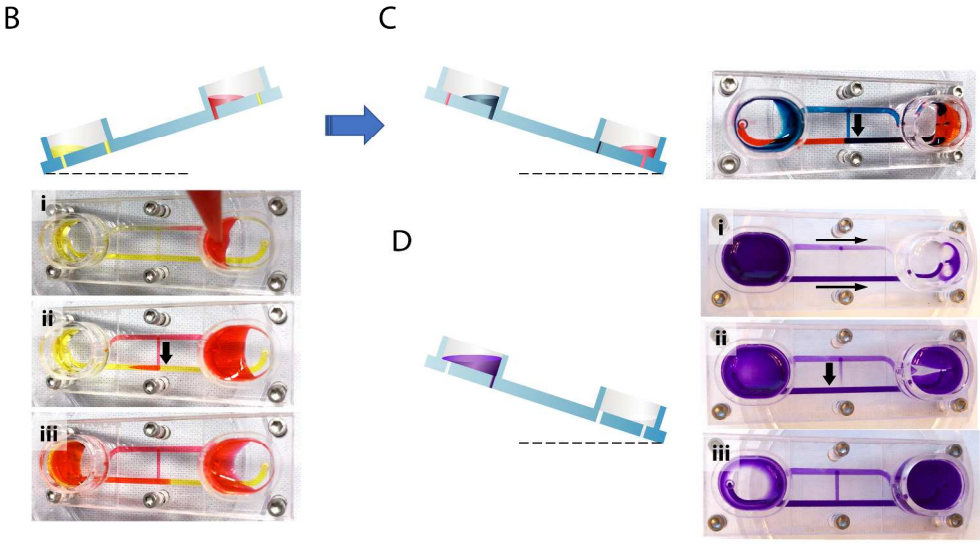

Figure 4 Computational and experimental analysis of fluid dynamics in a demonstration UniChip. (A) Magnitude (color coded) and direction (white arrow) of the velocity field were plotted at half depth plane of each channel (i). The simulated results verified the microfluidic channel design for the flow rate (ii) and shear stress (iii). Maximum flow velocities in different channels determined by measuring the linear velocity of a moving dye front. The results (n = 3) were within ±1~4% of the simulated values (iv). The flow direction was visualized with dyes. Red dye placed in one reservoir flows to the other reservoir through the top (inlet) and center channels (B). Once the device is flipped, blue dye is placed in the other reservoir and flows back to the initial reservoir through the inlet and center channels (C). Unidirectional flow is achieved within the center channel (black arrows in B-C). In cases where excessive fluid (purple dye) completely covers the passive valve and delays the liquid-air interface formation (D), fluid flows from one reservoir to the other through the top and the bottom channels (i, arrows), and starts to flow through the center channel when the interface begins to form. No backwards flow occurs during the whole period.

281x317mm (300 x 300 DPI)

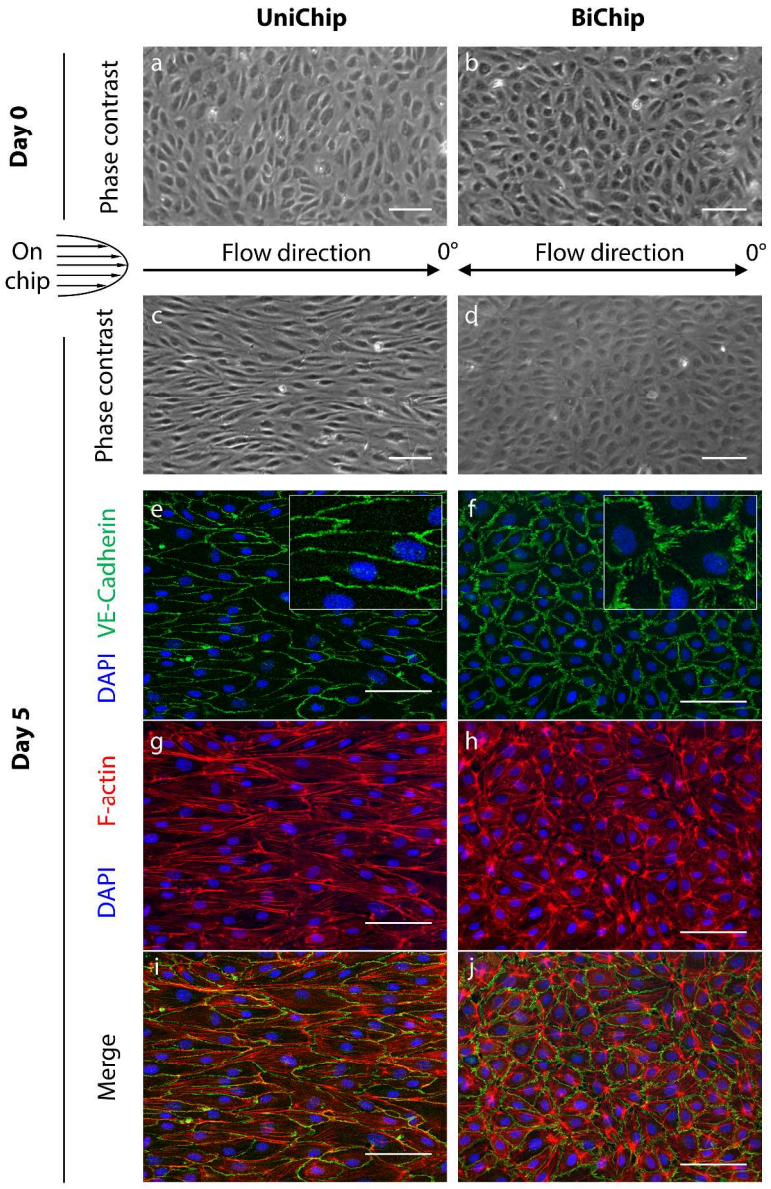

Figure 5 UniChip and BiChip perfusion elicit differential responses in cell morphology and distribution of VE-cadherin and F-actin. Phase contrast images of HUVECs on UniChips and BiChips before and 5 days after flow onset show clear cell elongation and realignment to the flow direction in UniChip perfused cells (c vs. a), yet no evident morphological change in BiChip perfused cells (d vs. b). Confocal microscopy reveals strong expression of VE-cadherin along the cell borders in both the UniChip and the BiChip cultured cells (e-f). Yet the distribution or network organization of VE-cadherin in the two culturese differs (zoomed-in insets in e-f). Immunostaining of F-actin with Alexfluor488-phalloidin shows differential F-actin morphology and orientation for the UniChip (g) and BiChip (h) groups. Merged mages of VE-cadherin and F-actin staining shows differential F-actin distribution in the two groups (i, j). Scale bar, 100 μm.

264x401mm (300 x 300 DPI)

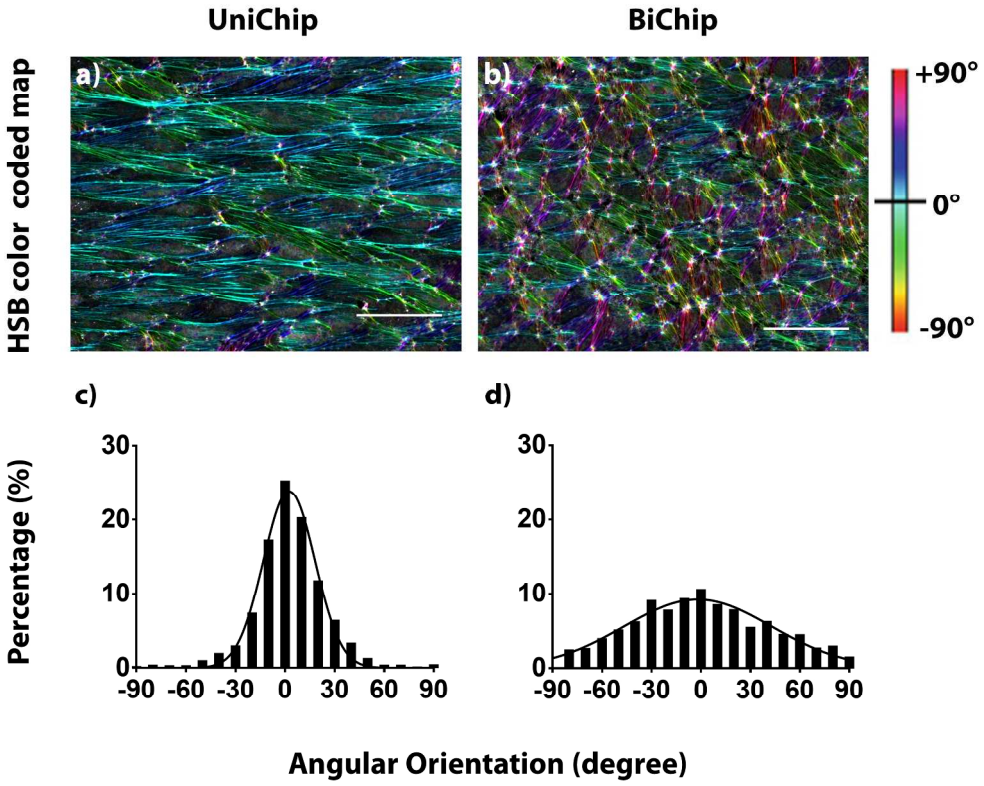

Figure 6 Visual and quantitative analysis of F-actin alignment in HUVECs cultured on UniChip and BiChip devices. The HSB (Hue: local orientation; Saturation: coherency; Brightness: from the original image) color coded maps derived from representative F-actin staining images reveal that a majority of F-actin in UniChip cultured cells aligned to the flow direction (a), while the spectrum of F-actin orientation in BiChip cultured cells is much broader (b). The quantitative analysis results of dominant F-actin orientation in 2000 cells of each group were summarized in c-d.

228x182mm (300 x 300 DPI)

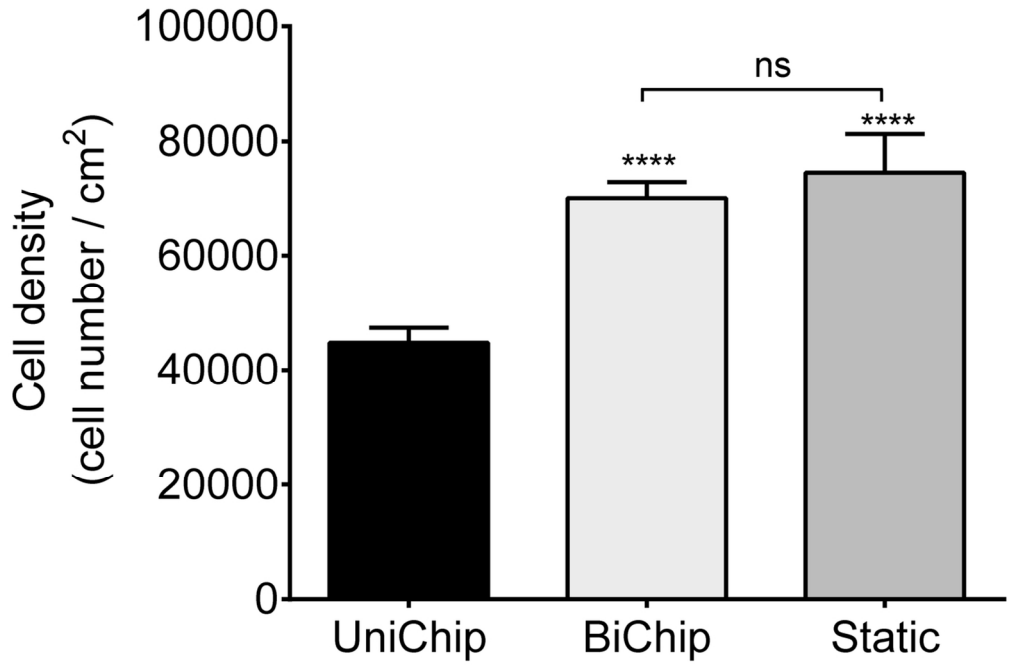

Figure 7 Endothelial cell density on UniChip, BiChip or in static culture. HUVECs were seeded onto cell inserts at a same density for all groups. UniChips and BiChips were assembled 24 hr later and operated for 5 days. Cells from 10 representative views (567μm × 567μm) for each group were then counted based on nuclear staining. Cells in all groups were confluent, yet those on UniChips showed significantly lower density than cells on BiChips or in static culture. Data are presented as mean ± SD. Significance by one-way ANOVA with Tukey's multiple comparisons test; **** $p < 0.0001$; ns, not significant.

117x78mm (300 x 300 DPI)

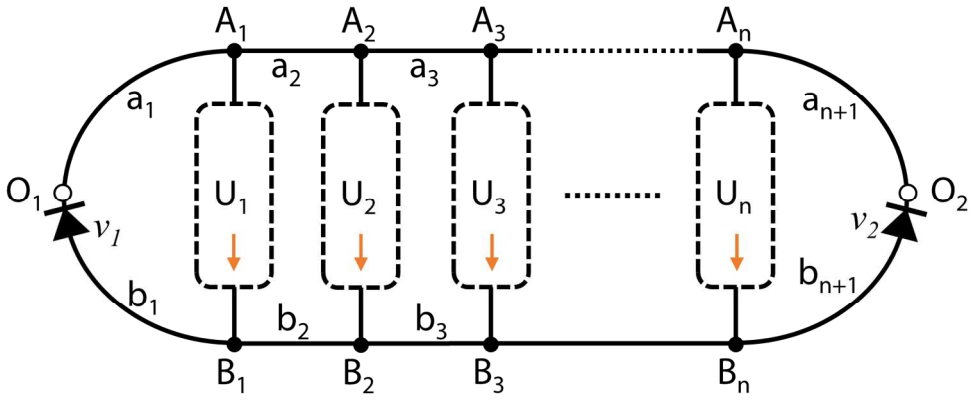

Figure 8 Schematic of UniChip design in general. The fluidic network includes a pair of inlet/outlet (O_1/O_2) for reciprocating flow input, one or more unidirectional channel network (UCN, U_1, U_2, …, U_n), and a supporting channel network (SCN, a_1, a_2, …, a_n, and b_1, b_2, …, b_n) including valving devices (v_1 and v_2). Fluid flows in UCN from inlets to outlets ($A_i \rightarrow B_i$, i = 1, 2, …, n).

152x63mm (300 x 300 DPI)

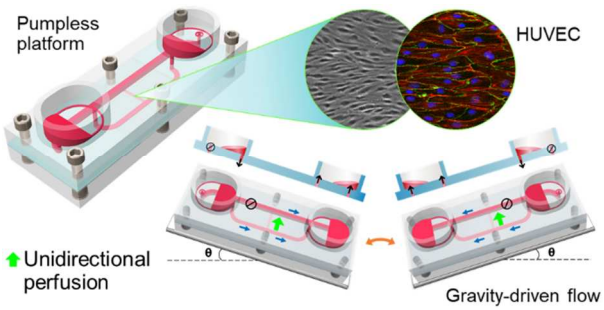

UniChip enables recirculating unidirectional perfusion with gravity-driven flow, facilitating reliable and cost-effective integration of shear stress-sensitive tissues into microphysiological systems.